



Preparation of La_2O_3 by ion-exchange membrane electrolysis of LaCl_3 aqueous solution[☆]

Deliang Meng, Qiuyue Zhao, Xijuan Pan, Ting'an Zhang^{*}

Key Laboratory of Ecological Metallurgy of Multi-Metal Intergrown Ores of Ministry of Education, School of Metallurgy, Northeastern University, Shenyang 110819, China

ARTICLE INFO

Article history:

Received 1 October 2018
Received in revised form
23 November 2018
Accepted 26 November 2018
Available online 8 April 2019

Keywords:

Lanthanum chloride
Membrane electrolysis
Lanthanum hydroxide
Lanthanum oxide
Current efficiency
Rare earths

ABSTRACT

The ion-exchange membrane electrolysis technology was applied inventively in the preparation of lanthanum hydroxide, after calcination, lanthanum oxide was obtained eventually. The effect of the concentration of lanthanum chloride solution on electrolytic product was mainly investigated. The phase composition, micro morphology, particle size and chlorine content of the product were characterized, respectively. Under the conditions of this work, the product that forms by electrolysis of LaCl_3 aqueous solution directly is $\text{La}(\text{OH})_3$. When the initial concentration of LaCl_3 changes from 0.1 to 0.5 mol/L, the current efficiency of $\text{La}(\text{OH})_3$ increases from 60% to 85%, the product roasted at 800 °C for 1.5 h is La_2O_3 , whose median particle size (D_{50}) is 10–20 μm , the mass fraction of chloride ion is less than 0.02 wt%. Additionally, the prepared La_2O_3 particles are porous and non-spherical particles, which are composed of small crystals with sheet structure.

© 2019 Chinese Society of Rare Earths. Published by Elsevier B.V. All rights reserved.

1. Introduction

Lanthanum oxide has excellent photoelectromagnetic properties, for this reason, lanthanum oxide is widely used to make new functional materials, such as catalysts, wear-resisting metal material, temperature sensor.^{1–6} Lanthanum hydroxide is the intermediate product of preparing lanthanum oxide. At present, the preparation methods of lanthanum hydroxide include precipitation method,^{7–9} hydro-thermal method,^{10–14} chemical reaction method,¹⁵ hydrolysis method,¹⁶ composite-hydroxide-mediated (CHM) methods,¹⁷ etc. Although each of these methods has many advantages, there is always room for improvement. The hydro-thermal method needs special reaction conditions and has high requirements for equipment, the reaction conditions of CHM methods are complex, etc. These deficiencies limit the extensive industrial application of these methods. Among them, owing to the

advantages of low cost, simple process and easy scale-up, the method of precipitation is widely used in industrial production, however, because the precipitation agents, such as oxalic acid and ammonium bicarbonate, are used in the process of precipitation, the amount of waste water containing ammonia nitrogen is large, which is very harmful to the environment.

Based on the technology of ion membrane electrolysis used in chlor-alkali industry and sewage treatment extensively,^{18–20} the idea proposed in this paper is that lanthanum oxide is prepared by electrolysis of lanthanum chloride aqueous solution, the simplified flowchart is shown in Fig. 1. Compared with the method of precipitation, this method does not need any additives, which reduces the chance of introducing other elements to the product. Meanwhile, the produced gases (Cl_2 and H_2) are of high purity, which can be collected respectively, and used as value-added products or for further synthesis of hydrochloric acid (HCl). The hydrochloric acid and the used electrolyte can be returned to the total production process of rare earth to achieve the purpose of recycling. Therefore, there is no waste discharge during the whole electrolysis process.

Based on the idea proposed above, this paper focuses on the effect of the concentration of lanthanum chloride solution on electrolytic product, and the phase composition and microstructure of the electrolytic product, as well as the micro morphology and particle size of the calcined product were analyzed. Besides, the

[☆] **Foundation item:** Project supposed by National Key R&D Program of China (2017YFC0210403-04; 2017YFC0210404), Liaoning Excellent Talent Cultivation Project (2015020591), the Young Creative Talents Project of Ordinary University in Guangdong Province (2015KQNCX157) and Hi-Tech Research and Development Program (863) of China (2010AA03A405).

^{*} Corresponding author.

E-mail address: zta2000@163.net (T.A. Zhang).

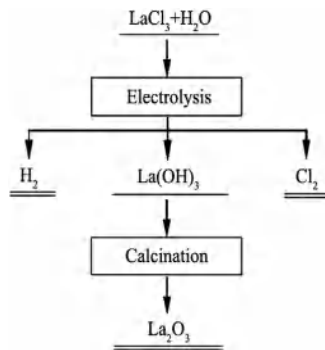


Fig. 1. Process flow chart of lanthanum oxide production.

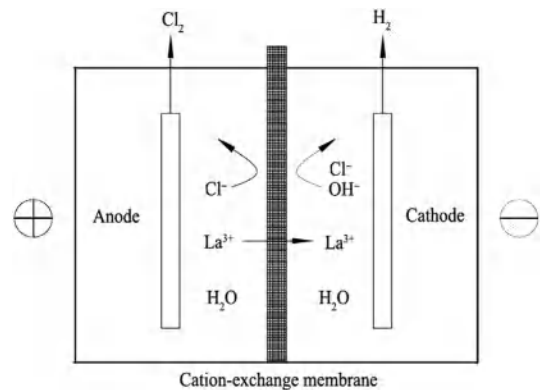


Fig. 2. Diagram of cationic membrane electrolysis.

current efficiency and energy consumption of the product were investigated.

2. Experimental

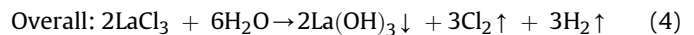
2.1. Reagents and main apparatus

$\text{LaCl}_3 \cdot n\text{H}_2\text{O}$ (analytic grade) was used to prepare the product. Water used in this work was de-ionized (homemade). Both cathode and anode were made of titanium sheets ($2\text{ cm} \times 3\text{ cm}$) coated with RuO_2 . The self-made ionic membrane electrolytic cell ($16\text{ cm} \times 6\text{ cm} \times 5\text{ cm}$) and cation-exchange membrane (CJMC-3) bought from Hefei Chem-Joy Polymer Materials Co., Ltd. were used in this work, and all the details of the ion-exchange membrane are shown in Table 1. Besides, various techniques were employed in this research, such as X-ray diffraction analysis (XRD, D8 Advance, Germany), scanning electron microscope (SEM, SU-8010, Germany), laser particle size analyzer (MS2000, Britain), inductively coupled plasma (ICP, Prodigy XP, USA), so that the phase composition, micro morphology, particle size of the product and the initial concentration of LaCl_3 in the electrolyte were analyzed, respectively.

2.2. Principle

Fig. 2 shows that the self-made electrolytic cell is divided by the cation-exchange membrane into two parts: anode chamber and cathode chamber, which are filled with electrolyte of LaCl_3 . When the direct current is switched on, in the anode chamber, La^{3+} can get through the cation-exchange membrane easily, while Cl^- cannot get through smoothly, and Cl^- is oxidized to Cl_2 on the anode surface. In the cathode chamber, H_2O is electrolyzed into H_2 and OH^- on the cathode surface, and OH^- combines with La^{3+} to form La(OH)_3 .

The reactions during the electrolysis are shown as follows:



2.3. Procedures

Firstly, the LaCl_3 aqueous solutions with concentrations of 0.1, 0.2, 0.3, 0.4 and 0.5 mol/L were added into both anode chamber and cathode chamber of the electrolytic cell, respectively, the initial pH of these solutions was about 5.0, and it was necessary to make sure that the liquid levels of both sides were of the same height.

Secondly, the electrolytic cell filled with electrolyte was moved into electro-thermostatic water cabinet to control the temperature, then the direct current was switched on, and the current was regulated to a constant of 1.2 A throughout the process of electrolysis. Meanwhile, the value of cell voltage was measured. In this study, due to the small experiment scale and little gas generation, considering the safety of the experimenters, the gases were not collected, but treated directly with a fume hood.

Finally, after 25 min of electrolysis at $25\text{ }^\circ\text{C}$, 4 cm of electrode distance, 200 mA/cm^2 of current density, the white precipitate was filtered and washed more than twice with de-ionized water, then was dried at $70\text{ }^\circ\text{C}$ overnight, the phase composition and micro morphology of the dried product were analyzed. Subsequently, the dried powders were calcined at $800\text{ }^\circ\text{C}$ in air for 1.5 h, after cooling, the phase information, the micro morphology and the particle size of the final product (La_2O_3) were analyzed. Besides, current efficiency and energy consumption of La(OH)_3 were monitored as an evaluation of different initial concentrations of LaCl_3 .

2.4. Related calculations

The electrolytic current efficiency (η) is the ratio of the electrodeposited mass to the theoretical mass. The theoretical mass of product can be obtained by Faraday's law. Therefore, η is represented as:

$$\eta = \frac{m_A}{m_B} \times 100\% = \frac{m_A}{I \cdot \Delta t \cdot M / (n \cdot F)} \times 100\% \quad (5)$$

Table 1
Performance parameters of the cation-exchange membrane (CJMC-3).

Performance parameters	Parameter values	Performance parameters	Parameter values
Moisture content (%)	35–45	Transference number	0.93
Thickness (mm)	0.17 ± 0.01	Bursting strength (MPa)	>0.35
Exchange capacity (mmol/g)	0.8–1.0	Membrane area resistance ($\Omega \cdot \text{cm}^2$)	2.5–3.5

In Eq. (5) above, η is cathode current efficiency (%), m_A and m_B are the actual mass and theoretical mass of the product, respectively (g), I stands for the value of current (A), Δt is the electrolysis time (s), M means the mole mass of the product (g/mol), n is equal to the number of electrons passed in the elementary electrode reaction, and F stands for Faraday's constant (about 96485 °C/mol).

The energy consumption (W) is defined as:

$$W = \frac{k \cdot V}{\eta} \quad (6)$$

Where, W stands for energy consumption (kW·h/kg), η is identical with η in Eq. (5), and V represents the value of cell voltage (V). Besides, k stands for the theoretical power consumption, which is used to describe the theoretical energy consumption and is required to produce per unit mass of product, the value of k is about 0.423 (kA·h/kg) in this work.

3. Results and discussion

3.1. Effect of initial concentration of LaCl_3 on phase compositions

XRD patterns of the products by electrolytic method are shown in Fig. 3. On the one hand, it is easy to see from Fig. 3 that the five diffraction lines below exhibit similar crystalline phases, which are identified as $\text{La}(\text{OH})_3$ (corresponding to JCPDS 36-1481). Additionally, when the initial concentrations are 0.1, 0.2 and 0.5 mol/L, respectively, the relative intensities of these peaks are much stronger than those of other peaks. The higher the peak of diffraction line is, the better the crystallinity of the product is. Additionally, the dried lanthanum hydroxide powders were calcined at 800 °C in air for 1.5 h, the phase information of the final product is shown as the diffraction curve at the top of Fig. 3. We can see from Fig. 3 that lanthanum hydroxide is completely transformed into lanthanum oxide after calcination, the equations of the reaction are as follows^{21,22}:

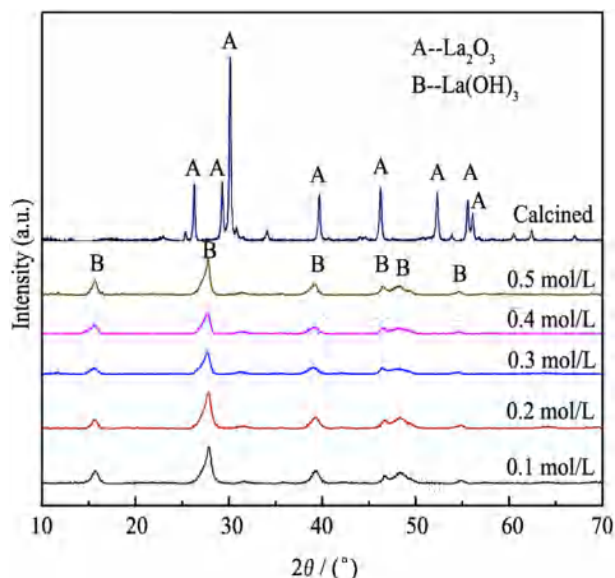


Fig. 3. XRD patterns of the samples before and after calcination.

On the other hand, no impurities are identified from XRD patterns of the products before and after roasting. After washing, the chlorine content of $\text{La}(\text{OH})_3$ is lower than 0.040 wt%, and that of La_2O_3 after roasting is lower than 0.018 wt%. According to GB/T 4154-2015, the chlorine content of lanthanum oxide products prepared by this method is lower than the national standard (0.02 wt% corresponding to La_2O_3 -4N5).

3.2. Effect of initial concentration of LaCl_3 on micro morphology

The morphology of the product is observed with SEM technique. The microstructures of the lanthanum hydroxide samples that form at different initial concentrations of LaCl_3 are shown in Fig. 4. Different initial concentrations may result in different microstructures. Obviously, when the initial concentrations are 0.1, 0.2 and 0.5 mol/L, respectively, the micro-structures of these particles are of great similarity, the surfaces of these crystals are covered with agglomerated particles (Fig. 4(a), (b) and (e), respectively), while the microstructures of the crystals obtained at the initial concentrations of 0.3 and 0.4 mol/L have similar characteristics, it is obvious that these crystals were composed of fibrous structures (Fig. 4(c) and (d)). According to the XRD patterns of the samples (Fig. 3), it may be inferred that the different relative intensities of diffraction lines might correspond to the different microstructures.

Some representative SEM micrographs of the lanthanum oxide samples are shown in Fig. 5. It is not difficult to see that the crystals after roasting have porous structure, and are composed of small particles with sheet structure. By contrast, the agglomerated particles that form at the initial concentration of 0.1 mol/L are more uniform (Fig. 5(a)), while the other morphology of the roasted products is very similar (Fig. 5(b–e), respectively). In the whole, the initial concentrations of LaCl_3 might have little influence on the morphology of the roasted particles. Additionally, the prepared lanthanum oxide crystals are non-spherical particles (Fig. 5(f)).

3.3. Effect of initial concentration of LaCl_3 on particle size of La_2O_3

It could be seen from the research above that $\text{La}(\text{OH})_3$ powders are formed at different initial concentrations of LaCl_3 , after calcination, La_2O_3 powders are obtained finally. The particle size distribution and median particle size (D_{50}) of La_2O_3 are shown in Figs. 6 and 7, respectively.

On the one hand, the conclusion drawn from Fig. 6 is that the particle size distributions of La_2O_3 are similar at different concentrations. When the concentrations are 0.4 and 0.5 mol/L, respectively, the uniformity of particle size is better than that of the particles obtained at the concentrations of 0.2 and 0.3 mol/L, but inferior to that of the sample obtained at the concentration of 0.1 mol/L. In addition, the product particle size distribution curve has two normal distribution peaks, and it can be known from the previous analysis that the product is pure substance. Therefore, the reason may be that the products are non-spherical particles, resulting in large differences in particle sizes in different directions, which is consistent with the results of microstructure analysis (Fig. 5(f)).

On the other hand, it can be seen from Fig. 7 that D_{50} of the particles is within 10–20 μm , which is in accordance with the provisions of lanthanum oxide national standard (GB/T 4154-2015). The large-size La_2O_3 can be used in many fields, such as the ceramics, polishing and glass industries. What's more, the curve in Fig. 7 indicates that the concentration has a great influence on the particle size. We can see that the median particle size of La_2O_3 decreases first and then increases with the concentration. The

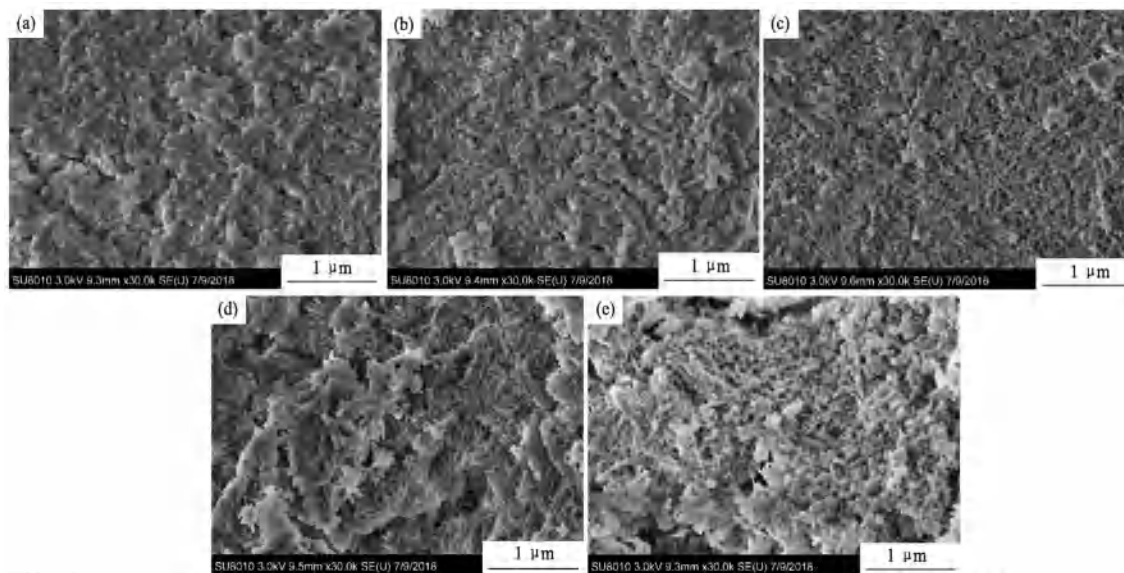


Fig. 4. SEM images of the lanthanum hydroxide samples formed at different initial concentrations of LaCl_3 . (a) 0.1 mol/L; (b) 0.2 mol/L; (c) 0.3 mol/L; (d) 0.4 mol/L; (e) 0.5 mol/L.

reason may be that the concentration had a great influence on the nucleation velocity of the crystal and the mass transfer velocity of the solute in the solution. When other conditions are certain, the growth rate of the crystal is greater than the nucleation rate at low concentration. As the concentration increases, the nucleation rate increases, which limits the growth rate because of the limited mass transfer speed, resulting in incomplete crystal development. Subsequently, the concentration continues to increase, both nucleation rate and growth rate of the crystal are improved, which allows the crystal to develop completely. Therefore, through the above analysis, it can be inferred that the median particle size (D_{50}) of the samples may be controlled by controlling the concentration of electrolyte.

3.4. Effect of initial concentration of LaCl_3 on current efficiency and energy consumption

The results given in Table 2 indicate that the production increases monotonically from 0.695 to 0.998 g with the initial concentration of LaCl_3 is elevated from 0.1 to 0.3 mol/L, and it remains about 1 g with the concentration is increased from 0.3 to 0.5 mol/L. In parallel, the average voltage decreases monotonically from 20.6 to 8.4 V, suggesting that the initial concentration has a great influence on the average voltage. According to the data in Table 2, it is easy to get the current efficiency and energy consumption of $\text{La}(\text{OH})_3$ by Eqs. (5) and (6) and the results are shown in Fig. 8. On the one hand, the current efficiency

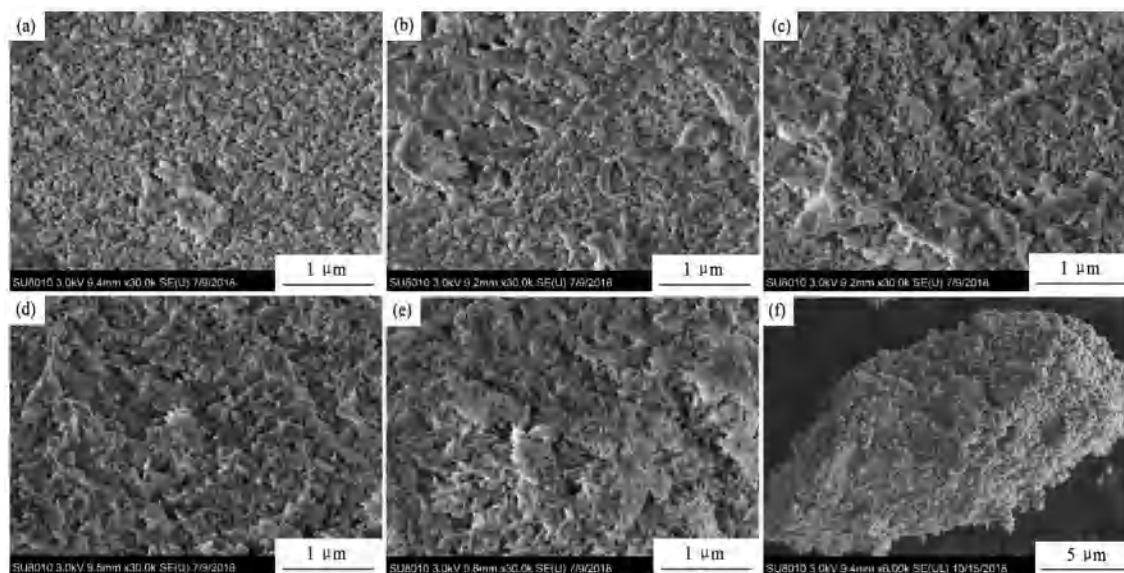


Fig. 5. SEM images of the lanthanum oxide samples calcined at 800 °C in air for 1.5 h at different initial concentrations of LaCl_3 . (a) 0.1 mol/L; (b) 0.2 mol/L; (c) 0.3 mol/L; (d) 0.4 mol/L; (e) 0.5 mol/L; (f) The big picture.

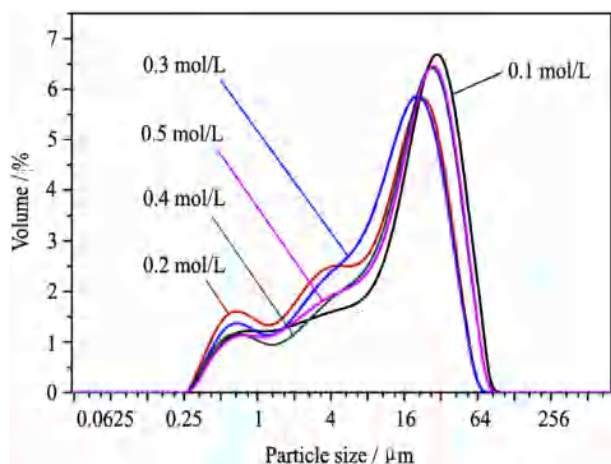


Fig. 6. Particle size distribution of La_2O_3 at different initial concentrations of LaCl_3 .

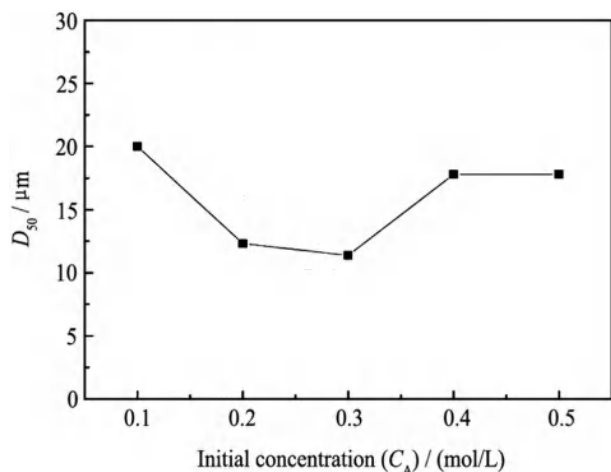


Fig. 7. Effect of the concentration of LaCl_3 on median particle size (D_{50}) of La_2O_3 .

is close to 60% at 0.1 mol/L, and when the initial concentration of LaCl_3 increases to 0.3 mol/L, the current efficiency reaches about 85%, and then it does not go up with the concentration; the energy consumption decreases monotonically from about 15 to 4 $\text{kW}\cdot\text{h}/\text{kg}$, the reason may be that the lower initial concentration has lower conductivity, which leads to higher energy consumption. On the other hand, according to the presented cathode and anode reaction of H_2 and Cl_2 , respectively, the theoretical electrolytic voltage of whole reaction will be 2.12 V. Although the voltage decreases as the concentration increases, the real electrolytic voltage is much higher compared with the theoretical value. The possible reasons include high resistance of the solution because of the large electrode distance, and high membrane area resistance of the ionic membrane, so the reduction of energy consumption will be studied in our future work.

Table 2

Effect of initial concentration of LaCl_3 on production of $\text{La}(\text{OH})_3$ and average voltage.

Initial concentration C_A (mol/L)	0.1	0.2	0.3	0.4	0.5
Production m (g)	0.695	0.844	0.998	1.005	1.002
Average voltage V (V)	20.6	14.9	11.9	9.1	8.4

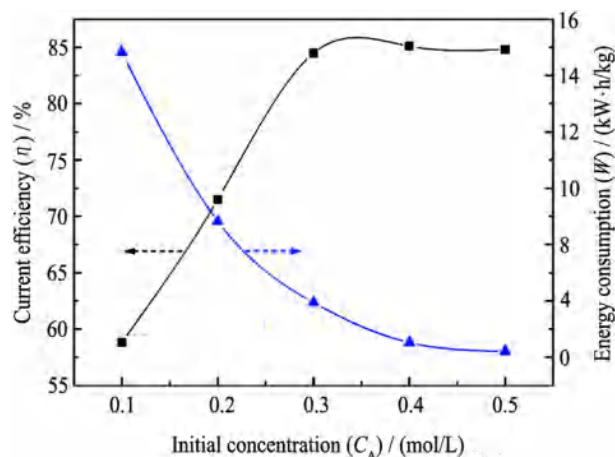


Fig. 8. Effect of initial concentration of LaCl_3 on current efficiency and energy consumption of $\text{La}(\text{OH})_3$.

4. Conclusions

The results of this research show that the new method of preparing the lanthanum oxide by electrolysis of lanthanum chloride aqueous solution is feasible, and the ion-exchange membrane electrolysis technology can be applied well in the preparation of lanthanum oxide. The influence of the initial concentration of LaCl_3 on the process of electrolysis was mainly studied, and the conclusions drawn at the conditions of this work are as follows:

According to the product characteristics analysis, the product formed by electrolysis of LaCl_3 aqueous solution directly is $\text{La}(\text{OH})_3$, whose chlorine content is lower than 0.04 wt%, the microstructure is fibrous and porous. After being roasted at $800\text{ }^\circ\text{C}$ for 1.5 h, La_2O_3 is obtained eventually, whose median particle size D_{50} is 10–20 μm , and the chlorine content is lower than 0.02 wt%. The crystals after roasting are porous and non-spherical particles, which are composed of small crystals with sheet structure. Additionally, the effect of the initial concentrations of LaCl_3 on the morphology of $\text{La}(\text{OH})_3$ and La_2O_3 is not obvious.

According to the results of calculation, when the initial concentration of LaCl_3 ranges from 0.1 to 0.5 mol/L, the current efficiency of $\text{La}(\text{OH})_3$ increases from about 60% to 85%, meanwhile, the energy consumption of $\text{La}(\text{OH})_3$ decreases from about 15 to 4 $\text{kW}\cdot\text{h}/\text{kg}$, respectively. Besides, when the concentration of LaCl_3 is more than 0.3 mol/L, the current efficiency will not increase with the concentration.

References

- Chen GR, Lei RS, Xu SQ, Wang HP, Zhao SL, Huang FF, et al. Effect of Li^+ ion concentration on upconversion emission and temperature sensing behavior of $\text{La}_2\text{O}_3:\text{Er}^{3+}$ phosphors. *J Rare Earths*. 2018;36(2):119.
- Binil PS, Anoop MR, Jisha KR, Suma S, Sudarsanakumar MR. Synthesis, spectral characterization, thermal and biological studies of lanthanide (III) complexes of oxyphebutazone. *J Rare Earths*. 2014;32(1):43.
- Kale SS, Jadhav KR, Patil PS, Gujar TP, Lokhande CD. Characterizations of spray-deposited Lanthanum Oxide (La_2O_3) thin films. *Mater Lett*. 2005;59(24–25):3007.
- Wang YJ, Chen JG, Yang J, Hao FF, Dan T, Yang YL, et al. Effect of La_2O_3 on granular bainite microstructure and wear resistance of hard facing layer metal. *J Rare Earths*. 2014;32(1):83.
- Gao YZ, Li YH, Zhang TS. Electron microscopic in-situ observation for preparation of ultrafine La_2O_3 nanophase powder. *J Rare Earths*. 1996;0(3):206.
- Liu J, Wang JQ, Zhao Z, Xu CM, Wei YC, Duan AJ, et al. Synthesis of $\text{La}_{x-1}\text{CoO}_3$ nanorod and their catalytic performances for CO oxidation. *J Rare Earths*. 2014;32(2):170.
- Kim SJ, Han WK, Kang SG, Han MS, Cheong YH. Formation of Lanthanum hydroxide and oxide via precipitation. *Solid State Phenom*. 2008;135:23.

8. Mendez M, Carvajal JJ, Marsal LF, Salagre P, Aguiló M, Díaz F, et al. Effect of the La(OH)₃ preparation method on the surface and rehydroxylation properties of resulting La₂O₃ nanoparticles. *J Nanoparticle Res.* 2013;15(3):1.
9. Kang JG, Kim YL, Cho DW, Sohn YK. Synthesis and physicochemical properties of La(OH)₃ and La₂O₃ nanostructures. *Mater Sci Semicond Process.* 2015;40:737.
10. Tang B, Ge JC, Zhuo LH. The fabrication of La(OH)₃ nanospheres by a controllable-hydrothermal method with citric acid as a protective agent. *Nanotechnology.* 2004;15(12):1749.
11. Wang Y, Liu SY, Cai Y, Deng SJ, Han BQ, Han R, et al. La(OH)₃:Ln³⁺ (Ln= Sm, Er, Gd, Dy, and Eu) nanorods synthesized by a facile hydrothermal method and their enhanced photocatalytic degradation of Congo red in the aqueous solution. *Ceram Int.* 2014;40(3):5091.
12. Jia G, Huang YJ, Song YH, Mei Y, Zhang LH, You HP. Controllable synthesis and luminescence properties of La(OH)₃ and La(OH)₃:Tb³⁺ nanocrystals with multifiform morphology. *Eur J Inorg Chem.* 2009;2009(25):3721.
13. Ding JW, Wu YL, Sun WL, Li YX. Preparation of La(OH)₃ and La₂O₃ with rod morphology by simple hydration of La₂O₃. *J Rare Earths.* 2006;24(4):440.
14. Mehdi MK, Sakineh A, Fateme A, Masoud SN. A controllable hydrothermal method to prepare La(OH)₃ nanorods using new precursors. *J Rare Earths.* 2015;33(4):425.
15. Li SC, Hu SJ, Du N, Fan JN, Xu LJ, Xu J. Low-temperature chemical solution synthesis of dendrite-like La(OH)₃ nanostructures and their thermal conversion to La₂O₃ nanostructures. *Rare Met.* 2015;34(6):395.
16. Li QT, Ni JS, Wu YQ, Du YN, Ding WZ, Geng SH. Synthesis and characterization of La(OH)₃ nanopowders from hydrolysis of Lanthanum carbide. *J Rare Earths.* 2011;29(5):416.
17. Hu CG, Liu H, Dong WT, Zhang YY, Bao G, Lao CS, et al. La(OH)₃ and La₂O₃ nanobelts—synthesis and physical properties. *Adv Mater.* 2010;19(3):470.
18. Du J, Su Y, Kong YZ, Wang JC. Control of impurity contents in brine for ion-exchange membrane electrolysis. *Chlor-Alkali Industry.* 2009;45(6):8.
19. Rozendal RA, Sleutels THJA, Hamelers HVM, Buisman CJN. Effect of the type of ion exchange membrane on performance, ion transport, and pH in biocatalyzed electrolysis of wastewater. *Water Sci Technol.* 2008;57(11):1757.
20. Simon A, Fujioka T, Price WE, Long DN. Sodium hydroxide production from sodium carbonate and bicarbonate solutions using membrane electrolysis: a feasibility study. *Sep Purif Technol.* 2014;127:70.
21. Wang XG, Wang ML, Song H, Ding BJ. A simple sol-gel technique for preparing lanthanum oxide nanopowders. *Mater Lett.* 2006;60(17–18):2261.
22. Hu HX, Qiu KQ. The imaging information implied in the graph of particles size distribution. *Phys Test Chem Anal (Part A:Physical Testing).* 2006;42(2):72.